Supplemental Figures

A Molecular Timer Couples Organism-Wide Temporal Identity to Developmental Checkpoints

Peipei Wu[1], Jing Wang[1], Brett Pryor[2], Isabella Valentino[2], David F. Ritter[3], Kaiser Loel[4], Justin Kinney[4], Sevinc Ercan[3], Leemor Joshua-Tor[1,5], Christopher M. Hammell[1,6,*]

[1]Cold Spring Harbor Laboratory, One Bungtown Road, Cold Spring Harbor, NY 11724
[2]Cold Spring Harbor Laboratory School of Biological Sciences, One Bungtown Road, Cold Spring Harbor, NY 11724
[3]New York University, 100 Washington Square East, New York, NY 10003
[4]Simons Center for Quantitative Biology, Cold Spring Harbor Laboratory, One Bungtown Road, Cold Spring Harbor, NY 11724
[5]Howard Hughes Medical Institute, W. M. Keck Structural Biology Laboratory, Cold Spring Harbor Laboratory, Cold Spring Harbor, NY 11724, USA
[6]Lead contact
*Correspondence: chammell@cshl.edu

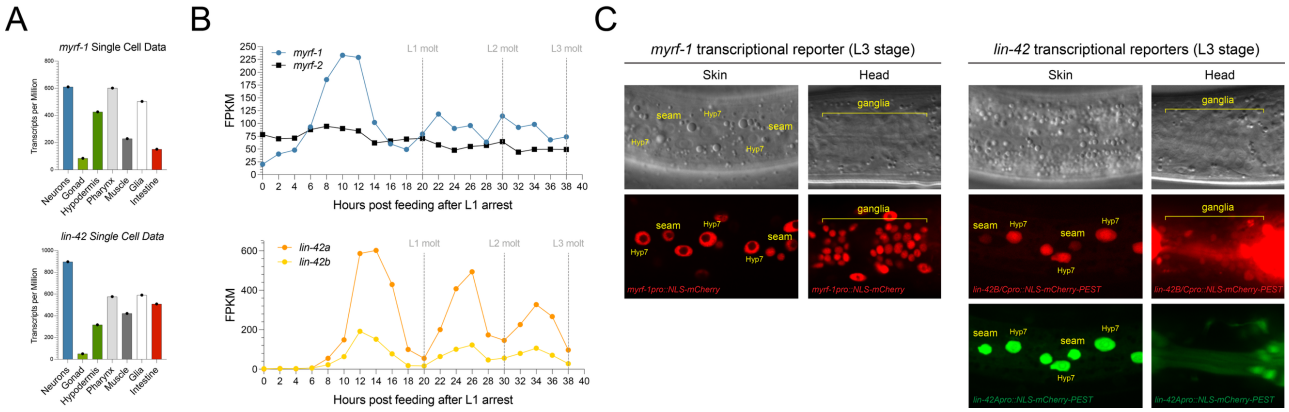

Figure S1 | MYRF-1 and LIN-42 expression dynamics across larval development. a, Single-cell RNA-seq analysis of L2-stage larvae (2) shows that *myrf-1* and *lin-42* transcripts are broadly expressed across most somatic cell types. **b,** Bulk RNA-seq time-course analysis (8) across post-embryonic development reveals that *myrf-1* and *lin-42* are transcribed in periodic, once-per-stage pulses. At each larval stage, *myrf-1* expression consistently precedes *lin-42* expression, establishing a reproducible phase delay between the two transcripts. **c,** Transcriptional reporter analyses demonstrate that this periodic, phase-ordered expression is transcriptionally driven and reiterated in multiple tissues, including hypodermal (skin) and neuronal cell types.

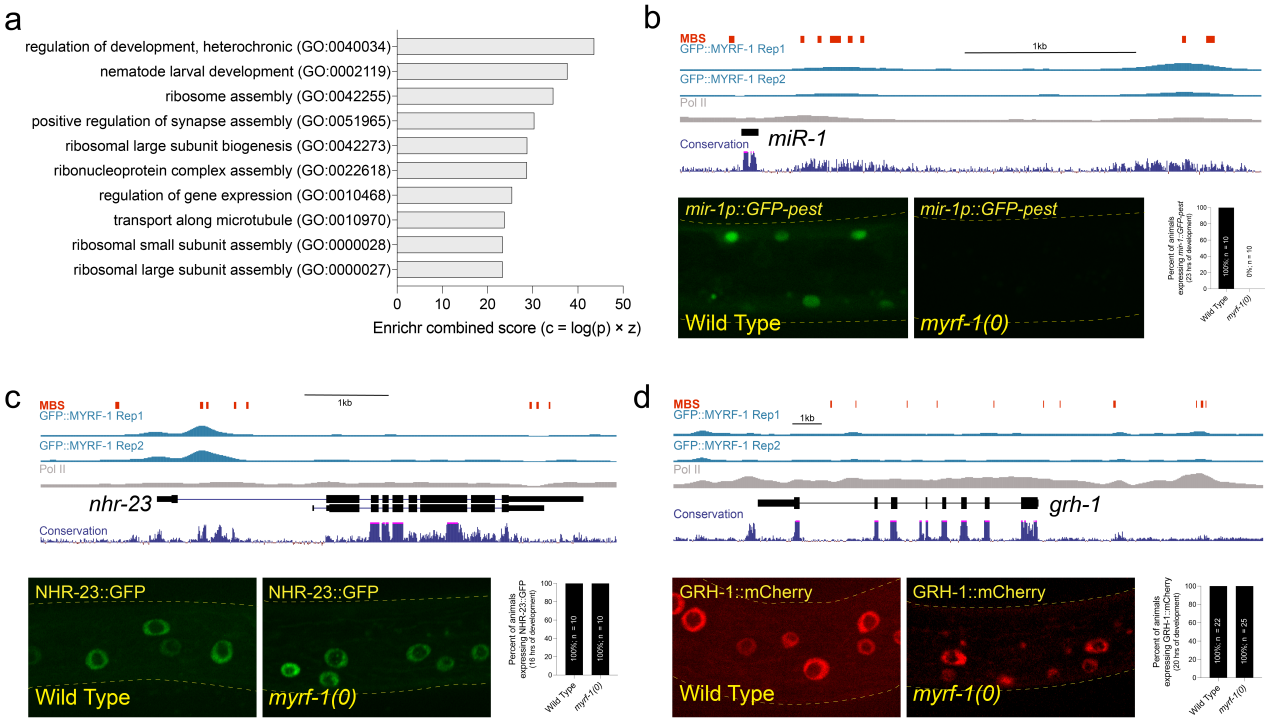

Figure S2 | MYRF-1 target enrichment classification and the dependency of MYRF-1 for MYRF-1 target genes expression. **a,** Gene Ontology (GO) enrichment analysis of MYRF-1-bound genes. **b,** MYRF-1 binds to the putative upstream regulatory regions of the *mir-1* gene, and the periodic expression of a *mir-1::GFP-pest* reporter requires MYRF-1 for expression. Red marks indicate the location of the MYRF-1 binding sequence illustrated in Fig. 1d. **c and d,** MYRF-1 is bound upstream of genes implicated in molting, including *nhr-23* and *grh-1*. Analysis of endogenously tagged alleles of these genes indicates that MYRF-1 is not required for their expression in hypodermal tissues.

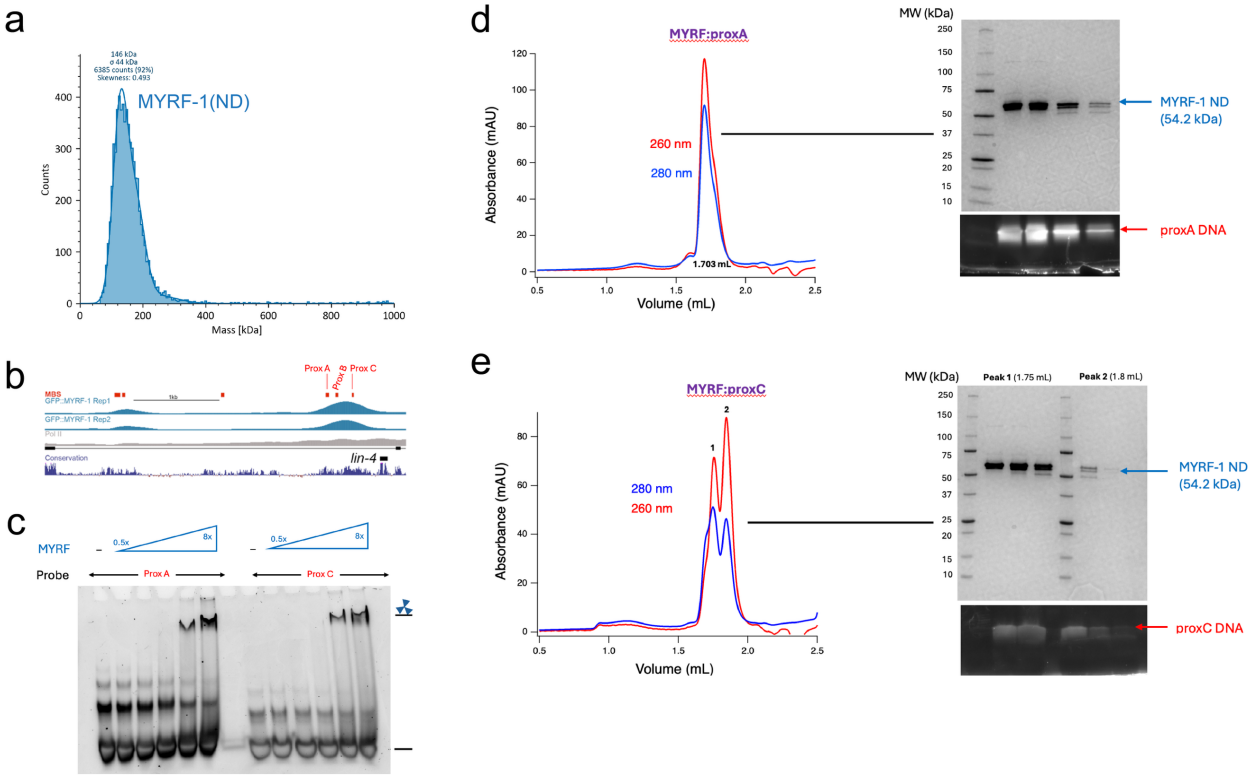

Figure S3 | MYRF-1 trimers bind Motif A and C within the *lin-4* proximal regulatory element. a, Mass photometry of recombinant MRYF-1 indicates that it forms a trimeric complex in solution with an apparent molecular weight of 146kD(+/- 44kD). This prediction is close to the calculated molecular weight of three MYRF-1(ND) polypeptides (3 x 54.2kD). **b,** Schematic of the *lin-4* locus showing distal and proximal MYRF-1 binding regions. Sequences that conform to the MYRF-1 consensus binding motif are indicated in red, with individual elements within the proximal region labeled A, B, and C. **c,** Electrophoretic mobility shift assays (EMSAs) showing that purified recombinant MYRF-1(ND) binds independently to the A and C elements of the *lin-4* proximal region. **d and e,** Size-exclusion chromatography demonstrates that MYRF-1(ND) binds the A and C elements as a homotrimer.

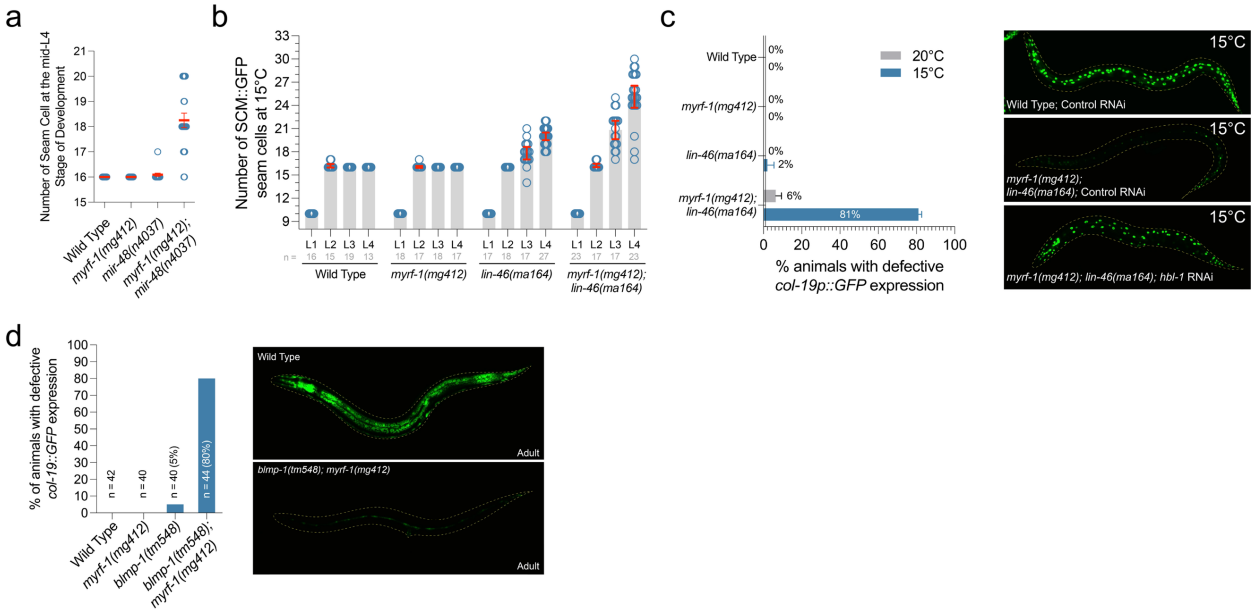

Figure S4 | Hypomorphic *myrf-1* alleles enhance heterochronic phenotypes of *mir-48, lin-46,* and *blmp-1*. a, *myrf-1(mg412); mir-48(n4097)* double mutants exhibit heterochronic seam cell linage phenotypes. **b,c,** LIN-46 post-translationally regulates the activity of the heterochronic transcription factor HBL-1(1). Strong loss-of-function alleles of *lin-46* cause mild heterochronic phenotypes that become more penetrant at lower temperatures(3). Combining the hypomorphic *myrf-1(mg412)* allele with *lin-46(ma164)* results in strongly enhanced heterochronic defects, including reduced expression of the adult-specific *col-19p::GFP* reporter and defects in adult alae formation. These phenotypes are fully suppressed by RNAi-mediated knockdown of *hbl-1*. Quantification: wild type + control RNAi, 100% normal *col-19p::GFP* expression (*n* = 43); *myrf-1(mg412); lin-46(ma164)* + control RNAi, 30% normal expression (*n* = 50); *myrf-1(mg412); lin-46(ma164)* + *hbl-1* RNAi, 100% normal expression (*n* = 25). **d,** BLMP-1 acts as a pioneer factor that primes multiple heterochronic microRNA loci for efficient transcription. The null allele *blmp-1(tm548)* exhibits mild heterochronic phenotypes, as assessed by *col-19p::GFP* expression. Combining *blmp-1(tm548)* with the hypomorphic *myrf-1(mg412)* allele results in strong misexpression of *col-19p::GFP* in adult animals.

Table S1 *myrf* genes interact with multiple heterochronic mutants to control temporal patterning patterning.

	Percentage of animals with *col19p::GFP* expression				
Genotype[a]	L3 molt	Details[b]	n=	L4 molt	n=
wild type	0%		20	100%	20
myrf-1(mg412) @20°C	0%		20	100%	22
myrf-1(mg412) @15°C	0%		20	100%	22
myrf-2(gk669)	0%		20	100%	20
myrf-1(mg412); myrf-2(gk669)	0%		20	100%	20
lin-42(n1089)	100%	100% (seam + hyp7)	24	100%	22
lin-42(n1089) myrf-1(mg412)	0%		20	100%	30
lin-42(n1089); myrf-2(gk669)	100%	100% (seam + hyp7)	20	100%	30
lin-42(n1089) myrf-1(mg412); myrf-2(gk669)	0%		22	100%	20
lin-42(ok2385)	96%	95.8% (16.7% seam only + 79.2% seam + hyp7)	24	100%	21
lin-42(ok2385) myrf-1(mg412)	60%	60% (15% seam only + 35% hyp7 only + 10% seam + hyp7)	20	100%	25
lin-42(csh83 (ΔMBD1))	0%		21	100%	30
lin-42(csh86 (ΔMBD2))	10%	10% (seam only)	20	100%	30
lin-42(csh83csh86 (ΔMBD1+2))	100%	100% (seam + hyp7)	22	100%	30
lin-42(csh89 (ΔPASB))	0%		23	100%	31

[a]All indicated strains harbor *ma105* V (encoding an integrated *col-19p::GFP* transcriptional reporter).

[b]The *col-19p::GFP* treanscrioinal reporter is normally expressed in the seam and hyp7 cells in adult animals. When *col-19p::GFP* is precociously expressed it can be expressed in each cell type. The descriptions in this column indicate the precocious expression pattern in each indicated genotype.

Table S2 Vulval developmental phenotypes of *lin-4* and *myrf-1(mg412)* mutant animals.

Strain	Genotype[a]	L4 vulval morphogenisis	Details[b]	n=	Adult Vulva[c]	n=	% Egl phenotype	n=
VT1367	wild type	100%	wild-type	30	100%	20	0%	25
HML1333	*myrf-1(mg412)*	100%	wild-type	40	100%	20	0%	35
HML006	*lin-4(e912)*	0%	No morphogenisis	21	0%	21	100%	32
HML1531	*lin-4(csh110)*	16%	16% have wild-type morphogenisis while the remainder have no or few divided P cells	25	0%	24	100%	60
HML1549	*lin-4(csh111) lin-4(csh110*	100%	wild-type	30	100%	21	0%	30
HML1564	*csh111)*	0%	No or few divided P cells	25	0%	21	100%	37
HML1544	*myrf-1(mg412) lin-4(csh110)*	24%	24% have wild-type morphogenisis while the remainder have no or few divided P cells	25	0%	23	100%	50

[a]Animals contain *maIs105*, which expresses an adult-specific, *col-19::GFP* reporter integrated on chromosome V.
[b]Status of vulval p-cell division and morphogenisis scored between L4.6 and L4.9 (Mok et al. 2015).
[c]Formation

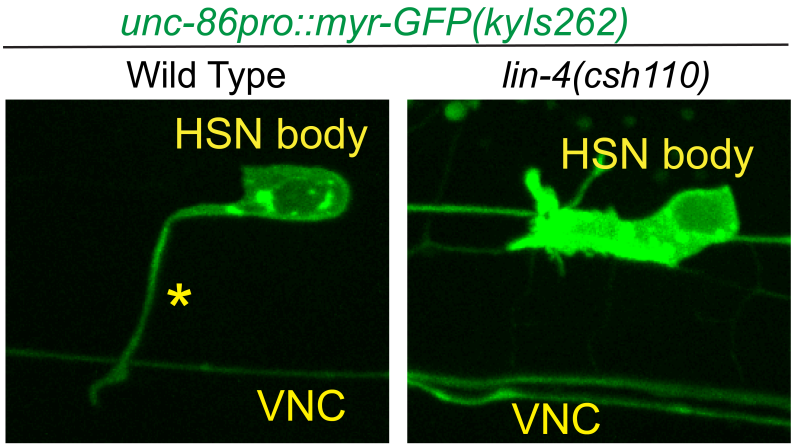

Figure S5 | Deletion of the proximal MYRF-1 binding site impacts the temporal regulation of hermaphroditic-specific neuron (HSN) axonal outgrowth. The development of the HSN neuron is temporarily regulated and well characterized (4). During the late-L3 stage, wild-type animals extend multiple neurites toward the ventral surface of the animal. By the early L4 stage and throughout adulthood, these projections project into the ventral nerve chord (VNC). HSN neurons in *lin-4(0)* animals fail to project and stabilize these axonal projections(7). When an *unc-86pro::myr-GFP* transgene was used to visualize HSN axonal projections, 100% of wild-type animals (n = 30) exhibited normal axonal projections. In contrast, of the 15 young adult *lin-4(csh110)* animals that also exhibited normal vulval morphogenesis, all failed to project a normal axon that reached the VNC.

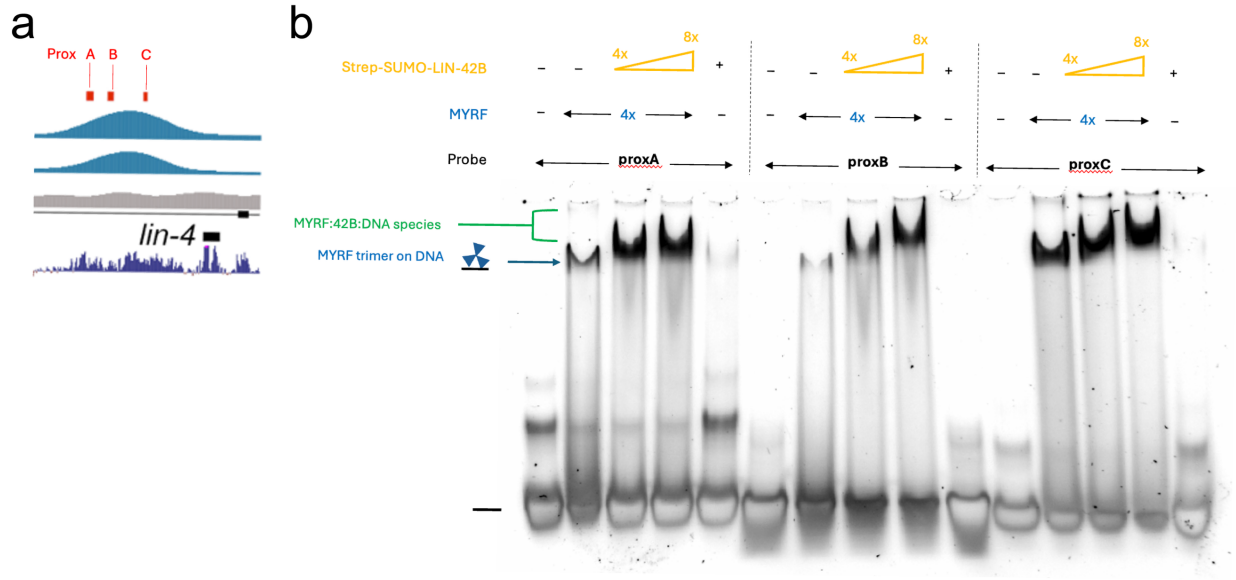

Figure S6 | LIN-42 super shifts individual MYRF-1 trimers bound to individual MYRF-1 binding sites within the *lin-4* proximal DNA fragment in EMSAs. a, Browser track showing the location of the *lin-4* proximal element binding sites labeled A, B, and C. **b,** Addition of recombinant LIN-42B into electrophoretic mobility shift assays containing MYRF-1(ND) and each of the *lin-4* proximal elements indicates that LIN-42 can supershift MYRF-1/DNA complexes for each element. Furthermore, LIN-42 does not appreciably bind any of the *lin-4* proximal element DNA fragments alone. In these experiments, binding reactions contained a 4x molar excess of MYRF-1(ND) to the probe, and LIN-42 was also at a 4x to 8x molar excess (compared to the probe). Images of the binding reactions for the *lin-4* proximal element Motif B are the same image shown in Fig. 3h.

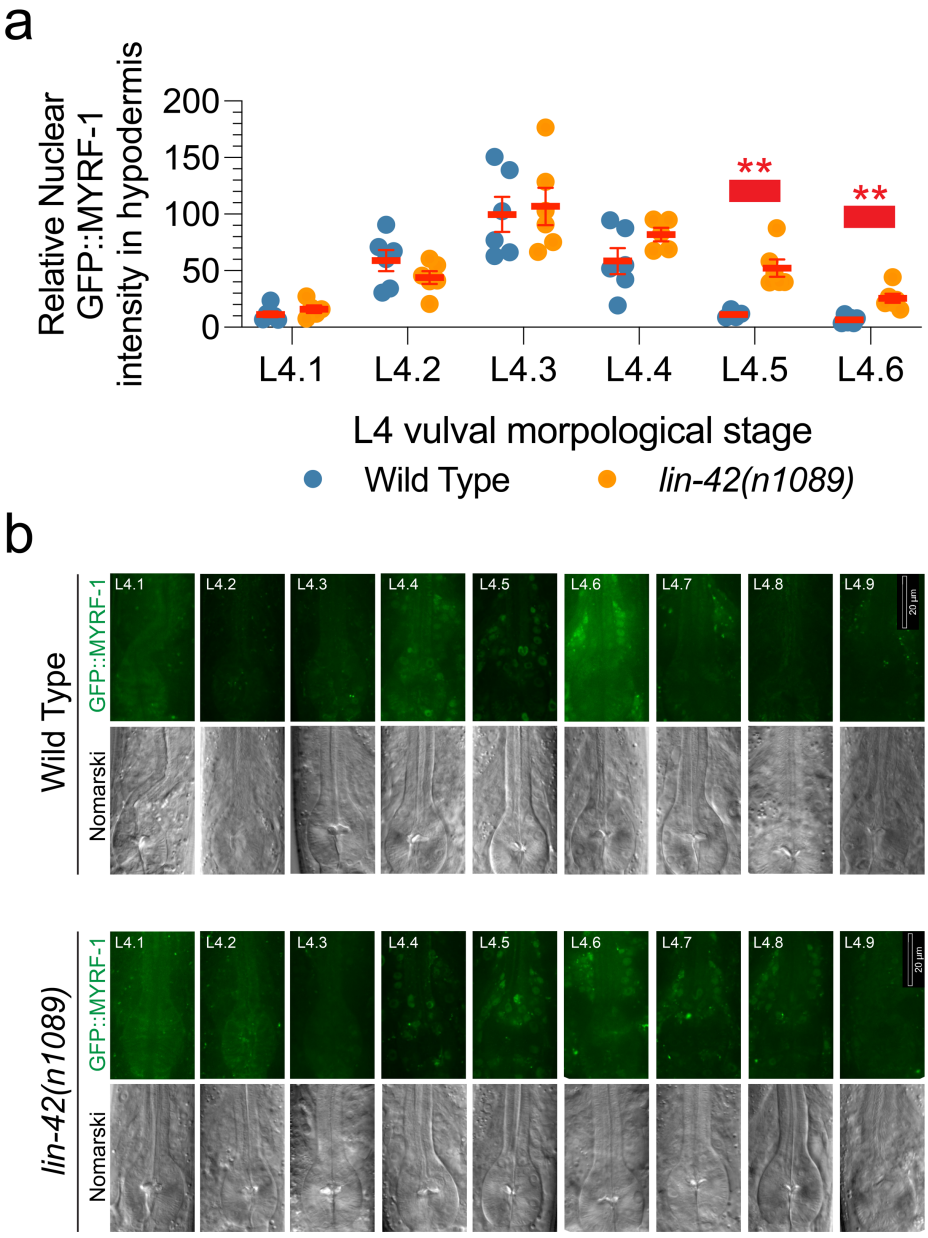

Figure S7 | Quantification of GFP::MYRF-1 nuclear dynamics in wild-type and *lin-42(n1089)* animals. a, Nuclear residency of GFP::MYRF-1 in hypodermal cells is significantly increased in *lin-42(n1089)* mutants at the L4.5 and L4.6 stages compared with wild type (Student's *t* test; $P < 0.01$). Each data point represents the mean background-subtracted nuclear fluorescence measured from three hypodermal cells in a single animal. **b,** The duration of nuclear GFP::MYRF-1 localization is also extended in neuronal cells in *lin-42(n1089)* mutants. The onset of nuclear GFP::MYRF-1 accumulation in neurons is delayed by approximately one L4 substage (~1 hour (5)), corresponding to the previously reported phase shift in *lin-4* transcription (6).

Table S3 A list of strains used in Wu et al. 2026

Strain name	Genotype	Source
HML1390	*myrf-1(csh82[GFP::MYRF-1]) II*	This study
VT1702	*maIs134[lin-4p::GFP + unc-119(+)]*	
HML1430	*maIs134[lin-4p::GFP + unc-119(+)]; myrf-1(ok3445)/(mIn1) II balancer*	This study
CGC152	*mir-48(umn59[mir-48p + SL1::EGL-13NLS::mScarlet-I::cMycNLS::Lox511I::let-858 3'UTR])*	
HML1472	*mir-48(umn59[mir-48p + SL1::EGL-13NLS::mScarlet-I::cMycNLS::Lox511I::let-858 3'UTR]); myrf-1(ok3445)/(mIn1) II balancer*	This study
HML87	*unc-119(ed3) III; maIs137 [let-7p::GFP + unc-119(+)]*	This study
HML1461	*unc-119(ed3) III; maIs137 [let-7p::GFP + unc-119(+)]; myrf-1(ok3445)/(mIn1) II balancer*	This study
HML734	*cshIs94[lin-42Ap::mCherry-pest; lin-42Bp::GFP-pest]*	This study
HML1423	*cshIs94[lin-42Ap::mCherry-pest; lin-42Bp::GFP-pest]; myrf-1(ok3445)/(mIn1) II balancer*	This study
HML780	*cshIs121 [mir-1p::GFP; col-42p::mCherry]*	This study
HML1442	*cshIs121[mir-1p::GFP; col-42p::mCherry]; myrf-1(ok3445)/(mIn1) II balancer*	This study
JDW29	*nhr-23(wrd8[nhr-23::GFP::AID*::3xFLAG]) I*	
HML1431	*nhr-23(wrd8[nhr-23::GFP::AID*::3xFLAG]) I; myrf-1(ok3445)/(mIn1) II balancer*	This study
RW12208	*grh-1(st12208[grh-1::TY1::EGFP::3xFLAG]) I*	Meeuse et al. 2023
HML1514	*grh-1(st12208[grh-1::TY1::EGFP::3xFLAG]) I; myrf-1(ok3445)/(mIn1) II balancer*	This study
VT1367	*maIs105[col-19p::GFP]*	Kinney et al. 2023
HML1333	*myrf-1(mg412); maIs105[col-19p::GFP]*	This study
HML1531	*lin-4(csh110); maIs105[col-19p::GFP]*	This study
HML1544	*myrf-1(mg412) lin-4(csh110); maIs105[col-19p::GFP]*	This study
VT1307	*mir-48(n4097); maIs105[col-19p::GFP]*	Hammell et al. 2009
HML1488	*myrf-1(mg412); mir-48(n4097); maIs105[col-19p::GFP]*	This study
VT1365	*let-7(mg279); maIs105[col-19p::GFP]*	Hammell et al. 2009
HML1490	*myrf-1(mg412); let-7(mg279); maIs105[col-19p::GFP]*	This study
HML0243	*wIs51[scm::GFP]*	This study
HML1443	*myrf-1(mg412); wIs51[scm::GFP]*	This study
HML1454	*lin-46(ma164) wIs51[scm::GFP]*	This study
HML1444	*myrf-1(mg412); lin-46(ma164) wIs51[scm::GFP]*	This study
VT1685	*lin-46(ma164); maIs105[col-19p::GFP]*	This study
HML1439	*myrf-1(mg412); lin-46(ma164); maIs105[col-19p::GFP]*	This study
HML1176	*blmp-1(tm548); maIs105[col-19p::GFP]*	This study
HML1457	*myrf-1(mg412)/mnC1; blmp-1(tm548); maIs105[col-19p::GFP]*	This study
HML1508	*lin-4(csh104)/nT1; maIs105[col-19p::GFP]*	This study
HML1549	*lin-4(csh111); maIs105[col-19p::GFP]*	This study
HML1564	*lin-4(csh110 cshI111); maIs105[col-19p::GFP]*	This study
HML1590	*lin-14(cc2891[LIN-14::GFP]) X*	This study
HML1589	*lin-4(e912); lin-14(cc2891[LIN-14::GFP]) X*	This study

HML1588	*lin-4(csh110); lin-14(cc2891[LIN-14::GFP]) X*	This study
OH16380	*nlp-45(ot1032[nlp-45::T2A::GFP::H2B]) X*	Sun and Hobert 2021
HML1245	*lin-4 (e912); nlp-45(ot1032[nlp-45::T2A::GFP::H2B]) X*	This study
HML1572	*lin-4 (csh110); nlp-45(ot1032[nlp-45::T2A::GFP::H2B]) X*	This study
OH11809	*otIs450[oig-1(fosmid)::SL2::GFP + rol-6(su1006)]*	Howel et al. 2015
HML1582	*lin-4(e912); otIs450[oig-1(fosmid)::SL2::GFP + rol-6(su1006)]; nlp-45(ot1032[nlp-45::T2A::GFP::H2B])*	This study
HML1576	*lin-4(csh110); otIs450[oig-1(fosmid)::SL2::GFP + rol-6(su1006)]*	This study
GR1395	*mgIs49 [mlt-10p::GFP::PEST + ttx-3::GFP] IV*	Russel et al. 2011
SR120	*myrf-1(mg412); mgIs49 [mlt-10p::GFP::PEST + ttx-3::GFP] IV*	Russel et al. 2011
HML902	*lin-42(n1089); mgIs49 [mlt-10p::GFP::PEST + ttx-3::GFP] IV*	This study
HML1452	*lin-42(n1089) myrf-1(mg412); mgIs49 [mlt-10p::GFP::PEST + ttx-3::GFP] IV*	This study
HML969	*lin-42(n1089); maIs105[col-19p::GFP]*	This study
HML1415	*lin-42(n1089) myrf-1(mg412); maIs105[col-19p::GFP]*	This study
HML1424	*lin-42(csh83 (∆MBD2/β-strand)); maIs105[col-19p::GFP]*	This study
HML1426	*lin-42(csh86 (∆MBD1/α-helix)); maIs105[col-19p::GFP]*	This study
HML1435	*lin-42(csh83csh86); maIs105[col-19p::GFP]*	This study
HML1393	*lin-42(n1089); myrf-1(csh82[GFP::MYRF-1]) II*	This study
HML1440	*lin-42(csh83csh86); myrf-1(csh82[GFP::MYRF-1]) II*	This study
HML1484	*myrf-1 (ns1102csh82 [degron::GFP::MYRF-1] II); otIs182 [eft-3pro::AtTIR1(F79G); myo-2pro::GFP]*	This study
HML1456	*icbsi123 [PDK72(srf-3;1;; delta-pes10;; syn21;; wrmScarlet-H2B;; p10 3'UTR + cb-unc-119)] II; wyIs592 [ser-2(prom3)::myr::GFP + odr-1p::RFP] III; myrf-1 (ns1102csh82 [degron::GFP::MYRF-1] II); otIs182 [eft-3pro::AtTIR1(F79G); myo-2pro::GFP] V*	This study
HML1418	*myrf-2(gk669); maIs105[col-19p::GFP]*	This study
HML1398	*myrf-1(mg412); myrf-2(gk669); maIs105[col-19p::GFP]*	This study
HML1420	*lin-42(n1089); myrf-2(gk669); maIs105[col-19p::GFP]*	This study
HML1413	*lin-42(n1089) myrf-1(mg412); myrf-2(gk669); maIs105[col-19p::GFP]*	This study
HML117	*lin-42(ok2385); maIs105[col-19p::GFP]*	This study
HML1386	*lin-42(ok2385) myrf-1(mg412); maIs105[col-19p::GFP]*	This study
HML1556	*icbSi123[PDK72[srf-3i1;; delta-pes10;; syn21;; wrmScarlet-o-H2B;; p10 3' UTR + cb-unc-119]] + myrf-1(ns1102csh82[degron::GFP::MYRF-1] II; wyIs592[ser-2(prom3)::myr::GFP + odr-1p::RFP] III; osIs182[eft-3p::AtTIR1(F79G); myo-2p::GFP] V*	This study

Table S4 | A list of reagents used for CRISPR genomic editing experiments outlined in this manuscript

Allele	Reagent Name	Sequence	Origin	Notes
csh111	Rev_2_ROR_2 sgRNA	UUGCACAAAUUGAGGUCAGU	Synthego	
	lin-4 PEAK sgRNA	CACGACCGGAAGAGCCUAAA	Synthego	
	DelDistal_RT	ttttttttccctttttcttgcacaaattgaggtcagttttaggctctt ccggtcgtgcaagaggaaatacaaa	Sigma Aldrich	HPLC Purfied
csh110	lin-4_proxMBS_5 sgRNA	UCCCCUGUGCCCAUUUGAAC	Synthego	
	lin-4_proxMBS_3 sgRNA	GUCGUUAUUCUUUUUUGCCG	Synthego	
	DelProxMYRFbs_RT	GGTCATTCGGTCGCTTCGTCGTTATTCTTTTT TGCCGTGGACGGCTGGTACACATACACATTC GTT	Sigma Aldrich	HPLC Purfied
csh82	myrf-1-Nterm sgRNA	AAUAUGUCUUACCUUUCAGA	Synthego	
	myrf-1_N_tagging II sgRNA	UCGAGCUCGGACCUUCUGAA	Synthego	
	GFP::MYRF-1 RT	tacccaataccaaagaaccgatactttagcacacttcgaa cATGAGTAAAGGAGAAGAACTTTTCACTGGA GTTGTCCCAATTCTTGTTGAATTAGATGGTGA TGTTAATGGGCACAAATTTTCTGTCAGTGGA GAGGGTGAAGGTGATGCAACATACGGAAAA CTTACCCTTAAATTTATTTGCACTACTGGAAA ACTACCTGTTCCATGGGTAAGTTTAAACATAT ATATACTAACTAACCCTGATTATTTAAATTTTC AGCCAACACTTGTCACTACTTTCTGTTATGGT GTTCAATGCTTCTCGAGATACCCAGATCATAT GAAACGGCATGACTTTTTCAAGAGTGCCATG CCCGAAGGTTATGTACAGGAAAGAACTATAT TTTTCAAAGATGACGGGAACTACAAGACACG TAAGTTTAAACAGTTCGGTACTAACTAACCAT ACATATTTAAATTTTCAGGTGCTGAAGTCAAG TTTGAAGGTGATACCCTTGTTAATAGAATCG AGTTAAAAGGTATTGATTTTAAAGAAGATGG AAACATTCTTGGACACAAATTGGAATACAAC TATAACTCACACAATGTATACATCATGGCAG ACAAACAAAAGAATGGAATCAAAGTTGTAAG TTTAAACATGATTTTACTAACTAACTAATCTGA TTTAAATTTTCAGAACTTCAAAATTAGACACA ACATTGAAGATGGAAGCGTTCAACTAGCAG ACCATTATCAACAAAATACTCCAATTGGCGAT GGCCCTGTCCTTTTACCAGACAACCATTACCT GTCCACACAATCTGCCCTTTCGAAAGATCCC AACGAAAAGAGAGACCACATGGTCCTTCTTG AGTTTGTAACAGCTGCTGGGATTACACATGG CATGGATGAACTATACAAAGAATTCCTGCAG CCCGGGGGATCCTCGAGCTCGGACttgttaAA AGgtaagacatattaaaaaaaaataggtt	PCR poduct	Gel Purified
csh86	PAS Helix_5	CCAGUCAAACACCCUGCCAC	Synthego	
	Whole PAS_3	GCUGAGAACUAUUAUGAAUA	Synthego	
	Delta PAS Helix RT	CGGATGTGATCTCCTCACCACCACCAGGCAT CCAGTCAAACACCCTGCCAAATAAGgtgagttc cgctatctcttcagtaaccttcttatcatccggcga	Sigma Aldrich	HPLC Purfied
csh83	deltaMBD_5 sgRNA	UCUGCGAGGAGGAUGUCCAG	Synthego	
	deltaMBD_3 sgRNA	CACGUCGGACUUGGUGUUGG	Synthego	
	delta-MBP RT	ATGTCCCGAGCTCCCCACCAGCGAAGCGTA CGACGACCAAGTCCGACGTGGAAAACGTGG CCTATCCAATCTCGG	Sigma Aldrich	HPLC Purfied

Table S5 | A list of the plasmids used in Wu et al. 2026

pCMH1986	pAD-Control
pCMH2463	pAD-MYRF-1(ND)
pCMH2503	pAD-MYRF-1(ND_mg412)
pCMH2487	pAD-MYRF-2(ND)
pCMH1987	pDB-Control
pCMH1967	pDB-LIN-42A
pCMH1968	pDB-LIN-42B
pCMH2540	pDB-LIN-42B-N-terminus
pCMH2537	pDB-LIN-42B-N-terminus - del_MBD1
pCMH2549	pDB-LIN-42A-del-MBD2
pCMH2513	pFL-MYRF-1(ND)
pCMH2607	pFL-LIN-42B

Table S6 | A list of probes used in EMSA experiments outlined in this study.

lin-4 proximal probe	Contains 3 predicted MYRF-1 binding sites. dsDNA	5'-CGCACTGAGAGAGAGGACAGACGAGAAGCGGAAGGCACACGCAGCAGAGCACGGAGGGACACGAGCGCGGCGCCCCGCAAGCCTTTCCGTGAGGCTGGCACCACCACCGCTTGGCGACGCGTCCCCGAAATAGTGTTAGGTGCCACAGAGACGTAGACCACCTCGCTCCCCTCTCATTTTTGCAGTAAGGGAGACTCGGCGTCTCGTCGACTTTTATTGTCTCTCACTGAGTATCTAGCCTTTCAGGGCGGCTGTTTAGGGAGAAGAAGCGGTGCGGAGTGAGCGCGGAGTAGAAGAGGATGAAAAACGAAACATAGAAAGAGAGAGAGAGGTCGTGCAATTTT-3'
lin-4 prox A: 48 bp	dsDNA	5'-AGAAGAGGATGAAAAACGAAACATAGAAAGAGAGAGAGAGGTCGTGCA-3'
lin-4 proxB: 44 bp	dsDNA	5'-AAGGGAGACTCGGCGTCTCGTCGACTTTTATTGTCTCTCACTGA-3'
Lin-4 proxC: 37 bp	dsDNA	5'-CTGAGAGAGAGGACAGACGAGAAGCGGAAGGCACACG-3'
AATT44: 44 bp	dsDNA	5'-AATTAATTAATTAATTAATTAATTAATTAATTAATTAATTAATT-3'

Bibliography

1. O. Ilbay, V. Ambros, Regulation of nuclear-cytoplasmic partitioning by the lin-28-lin-46 pathway reinforces microRNA repression of HBL-1 to confer robust cell-fate progression in C. elegans. *Development* **146** (2019).
2. J. Cao *et al.*, Comprehensive single-cell transcriptional profiling of a multicellular organism. *Science* **357**, 661–667 (2017).
3. A. S. Pepper *et al.*, The C. elegans heterochronic gene lin-46 affects developmental timing at two larval stages and encodes a relative of the scaffolding protein gephyrin. *Development* **131**, 2049–2059 (2004).
4. C. E. Adler, R. D. Fetter, C. I. Bargmann, UNC-6/Netrin induces neuronal asymmetry and defines the site of axon formation. *Nat Neurosci* **9**, 511–518 (2006).
5. D. Z. L. Mok, P. W. Sternberg, T. Inoue, Morphologically defined sub-stages of C. elegans vulval development in the fourth larval stage. *BMC developmental biology* **15**, 26 (2015).
6. B. Kinney *et al.*, A circadian-like gene network programs the timing and dosage of heterochronic miRNA transcription during C. elegans development. *Dev Cell* 10.1016/j.devcel.2023.08.006 (2023).
7. K. Olsson-Carter, F. J. Slack, A developmental timing switch promotes axon outgrowth independent of known guidance receptors. *PLoS Genet* **6** (2010).
8. D. h. Kim, D. Grün, A. van Oudenaarden, Dampening of expression oscillations by synchronous regulation of a microRNA and its target. *Nat Genet* **45**, 1337–1344 (2013).